HHS Public Access

Author manuscript

Neuropharmacology. Author manuscript; available in PMC 2020 November 01.

Published in final edited form as:

Neuropharmacology. 2019 November 01; 158: 107700. doi:10.1016/j.neuropharm.2019.107700.

Non-scaling regulation of AMPA receptors in homeostatic synaptic plasticity

Guan Wang[1,2], **Jia Zhong**[3], **Donovan Guttieres**[1], **Heng-Ye Man**[1,4,*]

[1]Department of Biology, Boston University, Boston, MA, USA

[2]School of Pharmaceutical Sciences, Tsinghua University, Beijing, China

[3]Harvard T.H. Chan School of Public Health, Harvard University, Boston, MA, USA

[4]Department of Pharmacology & Experimental Therapeutics, Boston University School of Medicine, Boston, MA, USA

Abstract

Homeostatic synaptic plasticity (HSP) as an activity-dependent negative feedback regulation of synaptic strength plays important roles in the maintenance of neuronal and neural circuitry stability. A primary cellular substrate for HSP expression is alterations in synaptic accumulation of glutamatergic α-amino-3-hydroxy-5-methyl-4-isoxazolepropionic acid receptors (AMPAR). It is widely believed that during HSP, AMPAR accumulation changes with the same proportion at each synapse of a neuron, a process known as synaptic scaling. However, direct evidence on AMPAR synaptic scaling remains largely lacking. Here we report a direct examination of inactivity-induced homeostatic scaling of AMPAR at individual synapse by live-imaging. Surprisingly, instead of uniform up-scaling, a scattered pattern of changes in synaptic AMPAR was observed in cultured rat hippocampal neurons. While the majority of synapses showed up-regulation after activity inhibition, a reduction of AMPAR could be detected in certain synapses. More importantly, among the up-regulated synapses, a wide range of AMPAR changes was observed in synapses of the same neuron. We also found that synapses with higher levels of pre-existing AMPAR tend to be up-regulated by lesser extents, whereas the locations of synapses relative to the soma seem not affecting AMPAR scaling strengths. In addition, we observed strong competition between neighboring synapses during HSP. These results reveal that synaptic AMPAR may not be scaled during HSP, suggesting novel molecular mechanisms for information processing and storage at synapses.

Graphical Abstract

*Correspondence should be addressed to: hman@bu.edu.

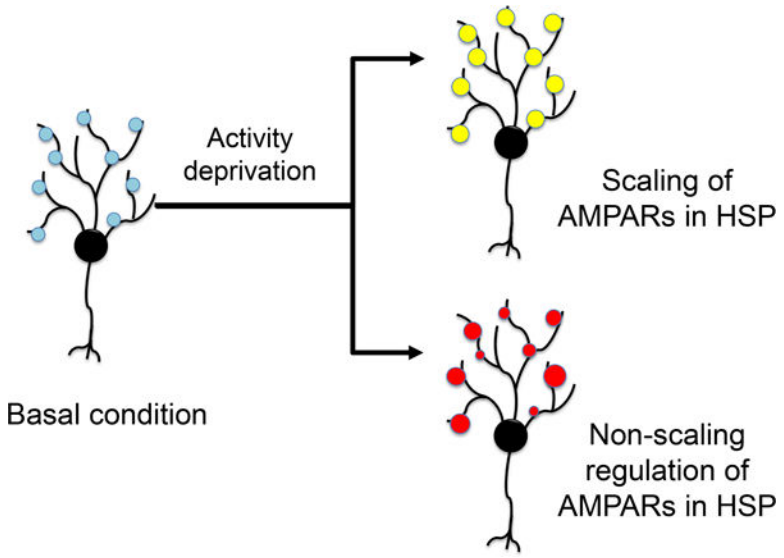

Keywords

AMPA receptor; Homeostatic synaptic plasticity (HSP); Synaptic scaling; Non-scaling regulation; AMPAR live-imaging

INTRODUCTION

In neurons, homeostatic plasticity serves to maintain a stable firing rate of action potentials. This can be achieved through adjustments in the strength of synaptic activity, neuronal excitability, neural cells connectivity, or the balance of excitation and inhibition (Turrigiano 2008, Pozo and Goda 2010, Turrigiano 2011, Vitureira et al. 2012, Fernandes and Carvalho 2016, Matsubara and Uehara 2016). Among these possibilities, regulation of synaptic strength has been the most extensively studied and is believed to be the most crucial measure in homeostatic regulation, also known as homeostatic synaptic plasticity (HSP) (Turrigiano et al. 1998, Davis and Bezprozvanny 2001, Davis 2006, Shepherd et al. 2006, Stellwagen and Malenka 2006, Turrigiano 2008, Hou et al. 2011, Hou et al. 2015). In addition to its roles in maintaining normal physiological brain functions, the contributions of HSP to neurological and psychiatric diseases, such as Alzheimer's disease and autism, have also been gradually revealed in recent years (Pratt et al. 2011, Blackman et al. 2012, Gilbert et al. 2016, Jewett et al. 2018, Lee et al. 2018, Styr and Slutsky 2018).

At the cellular level, inactivity-dependent homeostatic plasticity causes a simultaneous up-regulation of AMPAR at all synapses (Stellwagen and Malenka 2006, Sutton et al. 2006, Aoto et al. 2008, Hou et al. 2008, Ibata et al. 2008, Pozo and Goda 2010, Vitureira et al. 2012, Wang et al. 2012, Soares et al. 2013, Diering and Huganir 2018). It has been proposed that during the expression of homeostatic regulation, the amount of AMPAR added to each synapse is not by chance; rather, the response at individual synapse follows a common rule. In previous studies of HSP, the amplitudes of mEPSCs were often analyzed by cumulative plotting that ranks the miniature synaptic currents from the smallest to the largest

(Turrigiano et al. 1998, Wierenga et al. 2005, Stellwagen and Malenka 2006, Turrigiano 2008). The multiplicative pattern of the cumulative curves is thought to be a result from proportional increases in transmission strength of all synapses, namely, synaptic scaling. Synaptic scaling is considered an important cellular mechanism by which the relative strength of individual synaptic input can be maintained following homeostatic plasticity. It has been hypothesized that synaptic scaling of mEPSCs is due to the proportional addition of AMPAR to the entire synapse population of a neuron (Ibata et al., 2008; Pozo and Goda, 2010; Turrigiano, 2008). However, this hypothesis, though of fundamental significance, has not been validated by direct experimental evidence. We therefore directly examined AMPAR synaptic scaling in cultured neurons by a series of live-imaging experiments to compare changes of synaptic AMPAR amounts during HSP. To our surprise, we found that while AMPAR amount was increased in most synapses after neural activity deprivation, AMPAR accumulation did not show the expected pattern of scaling. Instead, among the synapse population, the extents of synaptic AMPAR increases showed a wide range of variation during HSP.

RESULTS

Live-imaging shows homeostatic up-regulation of synaptic AMPAR induced by neural activity deprivation

In order to analyze AMPAR accumulation at single synapse during HSP, we performed live-imaging on cultured hippocampal neurons expressing GFP-tagged (GFP-GluA1, GFP-GluA2) or pHluorin-tagged (pH-GluA1) AMPAR subunits, respectively. Two-wk-old hippocampal neurons were transfected for 3 days to express the target protein before experiments (Fig. 1A). Immunostaining of a synaptic marker PSD-95 indicated that the GFP-GluA1/2 or pH-GluA1 was successfully expressed and localized at the synaptic sites (GFP-GluA1: Fig. 1B; GFP-GluA2: Fig. S1A; pH-GluA1: Fig. S1B). High resolution live-cell imaging was performed before and after neural activity deprivation by application of sodium channel blocker tetrodotoxin (TTX, 2 μM) plus the N-methyl-D-aspartate (NMDA) receptor antagonist (2R)-amino-5-phosphonovaleric acid (APV, 50 μM) for 4 hours, a paradigm commonly used to induce HSP (Sutton et al. 2006, Aoto et al. 2008). The size and intensity of individual GFP-GluA1, GFP-GluA2 or pH-GluA1 punctum were measured and compared before and after the treatment. Consistent with studies of inactivity-induced HSP (Sutton et al. 2006, Aoto et al. 2008), 4 hr APV + TTX treatment increased GFP-GluA1 accumulation on overall synapse population by 43.28 ± 6.21% (n = 985 puncta of 30 neurons) (Fig. 1C). To examine whether the homeostatic changes in AMPAR follow the rule of scaling, we performed cumulative plotting that has been used to show the synaptic scaling in mEPSC amplitudes (Turrigiano et al. 1998, Stellwagen and Malenka 2006, Ibata et al. 2008). When the values of GFP-GluA1 puncta from control condition were multiplied with the average increase factor (1.43), we found that the cumulative plotting of this data set (the dashed black line) overlapped with the plot of neurons treated with APV+TTX (the red line), consistent with the pattern commonly used to indicate scaling (Fig. 1D). The plotting of ranked pre- and post-treatment GFP-GluA1 puncta values also showed a pattern of up-scaling (Fig. 1E).

AMPAR at different synapses are not regulated to the same extent during HSP

The lateral shift of cumulative plots of mEPSC amplitudes in HSP has been interpreted as a result of scaling in synaptic strength. It is hypothesized that during HSP, AMPAR amounts at individual synapses of a neuron/neural network are up- or down-regulated with the same proportion from its basal value prior to treatment (Turrigiano et al. 1998, Turrigiano 2008).

Surprisingly, when individual synaptic AMPAR puncta were compared prior to and after the inactivity treatment, we found that, rather than being uniformly up-regulated with the same percentage, they were apparently changed at random, varied levels. As is shown in Fig. 2, eight representative puncta on the same dendrite of a hippocampal pyramidal neuron exhibited different levels of changes in GFP-GluA1 puncta size and intensity (Fig. 2A – 2D). While most puncta showed increases (varied from 1.13 to 1.78), one punctum showed drastic decrease (#3, 0.42, Fig. 2D). Similar trends of changes were also observed in GFP-GluA2 (Fig. S2) and pH-GluA1 (Fig. S3). These findings revealed that synaptic AMPAR accumulation may not be proportionally up-regulated at individual synapse, suggesting a lack of AMPAR synaptic scaling during homeostatic regulation.

AMPARs at individual synapses are up-regulated to a wide range of degrees during HSP

To further examine the synaptic variations of AMPAR homeostatic regulation, we analyzed a large number of GFP-GluA1, GFP-GluA2 and pH-GluA1 puncta from different transfected neurons incubated with vehicle control or APV + TTX for 4 hr. As a system control for possible variations in fluorescence intensity during the imaging process, we fixed the transfected cells and subjected them to the same experimental procedure (Fig. 3A). The standard deviations (SD) and ranges of synaptic GFP-GluA1, GFP-GluA2 or pH-GluA1 amount changes before and after the treatment were used as indictors to measure the variations of synaptic AMPAR subunits changes (Fig. 3A – 3F).

We found that the basal activity of live neurons in vehicle control produced higher variations of synaptic AMPAR changes (SD = 0.17, puncta = 952, neurons = 29) than in system control (SD = 0.09, puncta = 967, neurons = 28) (Fig. 3A, 3B). However, inconsistent with the prediction of synaptic scaling theory, treatment with APV+TTX led to a wide range of changes in GFP-GluA1, GFP-GluA2 or pH-GluA1 puncta intensity (GFP-GluA1: Avg = 1.43, SD = 0.40, N = 985 puncta of 30 neurons; GFP-GluA2: Avg = 1.45, SD = 0.54, N = 956 puncta of 29 neurons; pH-GluA1: Avg = 1.29, SD = 0.34, N = 1012 puncta of 32 neurons) (Fig. 3C – 3E). A minor level of fluorescence bleaching was observed in the system and vehicle controls, reflected by the slight decreases in GFP-GluA1 fluorescence intensity in the post-4 hr imaging (System control: 0.91 ± 0.07; Vehicle control: 0.93 ± 0.12) (Fig. 3A and 3B). The ranges of HSP changes in APV+TTX treated neurons were significantly different from those detected in vehicle or system control (Fig. 3F).

To further confirm that HSP regulation of AMPAR is in a scattered, non-scaling pattern, we again made the conventional cumulative plots for homeostatic scaling analysis. Using the same data sets of Fig. 3C, 3D and 3E, we plotted the puncta intensity of GFP-GluA1, GFP-GluA2 or pH-GluA1 in ranked and unranked manners. In line with our observations in Fig. 3, even if generated from the same data set, we found that the ranked and unranked

cumulative plotting produced two very different distribution patterns (Fig. 4A – 4C). The ranked plotting generated a smooth and parallel-shifted curve (the black line) relative to the ranked pre-treatment curve (the blue line), seemingly indicating the scaling effect. However, the unranked data of synaptic AMPAR changes produced a highly-scattered pattern (the color dots) (Fig. 4A – 4C), indicating a non-scaled regulation in AMPAR synaptic accumulation. Similar scattered patterns of synaptic AMPAR were also observed in another classical plotting way to show synaptic scaling in HSP (Fig. S4 A – S4C). We also compared the extent of homeostatic regulation on different AMPAR subunits and the surface receptors. We found that GFP-GluA1, GFP-GluA2 and pH-GluA1 showed similar overall changes in response to APV+TTX 4h treatment (Fig. 4D). To determine whether the non-scaling occurs at individual neuron level, we plotted AMPAR puncta changes by cells. While control cells showed only minimal variations among the receptor puncta (Fig. 5A), neurons treated with APV+TTX had a wide range of variations for GFP-GluA1, GFP-GluA2 and pH-GluA1, respectively (Fig. 5B – 5D).

The basal levels of AMPAR at individual synapses are negatively correlated with the strength of HSP

To examine factors that may determine the extent of homeostatic alterations in synaptic AMPAR accumulation, we first evaluated the role of basal synaptic AMPAR level prior to HSP induction. In vehicle control cells, the basal level of AMPAR puncta had no relationship with the post-treatment synaptic AMPAR intensity (puncta = 952, $P = 0.10$, Fig. 6A). In contrast, a clear negative correlation was detected between the pre-treatment basal level of GFP-GluA1, GFP-GluA2 or pH-GluA1 with the homeostatic changes in receptor puncta intensity (GFP-GluA1: puncta = 985, $P < 0.0001$; GFP-GluA2: puncta = 956, $P < 0.0001$; pH-GluA1: puncta = 1012, $P < 0.0001$) (Fig. 6B – 6D). These results indicate that synapses containing less AMPARs tend to show stronger homeostatic responses, whereas synapses with more AMPARs have relatively weaker HSP responses. We next analyzed the potential role of AMPAR punctum location along the dendrite shaft in its homeostatic response. Interestingly, similar extents of homeostatic response were observed on AMPAR puncta located at different distances relative to the some (Vehicle control: puncta = 952, $P = 0.91$; GFP-GluA1: puncta = 985, $P = 0.39$; GFP-GluA2: puncta = 956, $P = 0.91$; pH-GluA1: puncta = 1012, $P = 0.17$) (Fig. 6E – 6H).

Neighboring synapses compete for AMPAR recruitment during HSP

Two closely located synapses on the same dendrite have been shown to compete for cellular machinery during Hebbian-type synaptic plasticity, resulting in opposite patterns of regulation (Govindarajan et al. 2006, Govindarajan et al. 2011). We wondered whether similar mechanisms exist in homeostatic plasticity as well. To explore this possibility, we analyzed around 100 pairs of closely distributed GFP-GluA1, GFP-GluA2 or pH-GluA1 puncta with varied distances between each other (Fig. 7A – 7D). We found that among these puncta pairs, the differences in synaptic AMPAR homeostatic response are negatively correlated to their separation distances (GFP-GluA1: n = 91 pairs from 10 neurons, $P = 0.02$; GFP-GluA2: n = 107 pairs from 11 neurons, $P = 0.009$; pH-GluA1: n = 101 pairs from 12 neurons, $P = 0.01$) (Fig. 7B – 7D), indicating that AMPARs may be favorably recruited to one of the neighboring synaptic sites during HSP.

Furthermore, previous studies suggested that synapses at the branching sites of dendritic arbors serve as “material depot” in which functional molecules or organelles are accumulated (Horton and Ehlers 2003, Horton et al. 2005). It has also been found that the homeostatic spine scaling is constrained to the dendritic branching region (Barnes et al. 2017). If AMPARs are delivered along the dendrites to synapses during HSP, it is possible that the receptor protein is temporarily deposited at a strategic location to secure continuous supply to more distal locations. We therefore measured the AMPAR puncta located at the dendrite branching sites in comparison with those at the nearby synaptic sites along the dendritic shaft. Indeed, we found that the GFP-GluA1, GFP-GluA2 or pH-GluA1 puncta at the dendrite branching sites were up-regulated to a significantly higher level during HSP (GFP-GluA1: n = 159 puncta of 19 neurons, $P < 0.001$; GFP-GluA2: n = 143 puncta of 18 neurons, $P < 0.05$; pH-GluA1: n = 165 puncta of 20 neurons, $P < 0.01$) compared to the rest of puncta population at non-branching sites of the same cells (Fig. 7E – 7H).

DISCUSSION

By utilizing high-resolution live-imaging of GFP-tagged AMPAR subunits, we analyzed the homeostatic up-regulation of AMPARs at individual synapses. Most importantly, we found that during HSP, changes in AMPAR synaptic accumulation, while showing up-regulation in most synapses, did not scale up uniformly among the synapse population. Under activity deprivation by APV + TTX treatment, individual AMPAR puncta at the synapses of a neuron show a wide range of changes, including down-regulation, relative to the pre-treatment basal conditions.

Synaptic scaling is originally derived from the observation that when the amplitudes of mEPSCs are plotted cumulatively, HSP results in a lateral shift of the curve (Turrigiano et al. 1998, Stellwagen and Malenka 2006, Sutton et al. 2006, Aoto et al. 2008, Ibata et al. 2008). The lateral shift of the cumulative probability curve by this mathematical analysis has been assumed to reflect a multiplicative nature of homeostatic effect on mEPSCs, which has been considered the evidence for synaptic scaling, i.e., activities of all synapses are regulated proportionally and identically. Although the limitations of this analysis method have been previously pointed out and non-multiplicative homeostatic regulation has been reported, it remains the most widely used model for synaptic scaling (Echegoyen et al. 2007, Kim et al. 2012). Because HSP is expressed through synaptic accumulation of AMPARs, the net addition of AMPARs to every synapse is assumed to be of the same in percentage or proportion, i.e., in a manner of scaling. However, this hypothesis has not been directly examined so far. Our findings suggest a non-scaling homeostatic regulation in synaptic expression of AMPARs. To our surprise, when we analyzed our data with cumulative plotting as conventionally used for mEPSC analysis, we observed the same pattern considered as scaling, suggesting that the “synaptic scaling” might be an analytical artifact. Therefore, HSP is not expressed by “scaled” changes in AMPAR amount at individual synapses of a neuron.

Studies have shown that homeostatic plasticity regulates synaptic functions not only globally at the cellular and circuit levels, but also locally at single synapses (Hou et al. 2008, Beique et al. 2011, Hou et al. 2011). Consistent with this, selective inhibition of synaptic activity

without interfering the postsynaptic neuronal firing is sufficient to trigger HSP (Fong et al. 2015). The input-specific induction of HSP demands a non-uniform regulation in synaptic strength during HSP.

Synaptic scaling is expected to be of vital functional significance in information processing in the brain. In a neural network, scaling allows individual synapses to maintain their relative strengths, which is believed to be crucial for the retention of memory. Although our results show a non-scaling homeostatic regulation, indicated by a lack of multiplicative up-regulation of individual AMPAR puncta, interestingly, we found that the overall populational changes in synaptic AMPAR nevertheless follow a general trend of scaling, rather than the completely random individual changes (Fig. 4 A – C; Fig. S4). It is possible that for a neuron or a neural circuit, though perfect scaling does not exist or is difficult to achieve, there seems to be a certain degree of scaling fidelity, which may be a biological variable that is either cell/network-specific or subject to developmental or activity-dependent regulation. Therefore, the consistency and quality of memory information over long-term storage may be affected by the scaling fidelity.

We further show that the changes of synaptic AMPAR in HSP are significantly correlated with the pre-existing amount of the receptors. The synapses with the lowest 10% of pre-existing AMPAR showed drastically higher up-regulation capability (GFP-GluA1: 171.93 ± 6.21%; GFP-GluA2: 175.55 ± 7.69%; pH-GluA1: 149.15 ± 5.49%) than the top 10% synapses (GFP-GluA1: 108.63 ± 2.28%; GFP-GluA2: 120.44 ± 4.94%; pH-GluA1: 127.28 ± 3.18%) (Fig. 6B – 6D), comparing with the medium average increases of the entire population. However, intriguingly, among the 10% of synapses with decreased AMPARs, a pattern of relatively uniform change was observed, indicating a complicated cellular mechanism contributing to AMPAR down-regulation.

During Hebbian-type long-term potentiation (LTP), neighboring synapses compete for the cellular machinery needed for protein synthesis from the same “material pools” in dendrites (Govindarajan et al. 2006, Govindarajan et al. 2011). Similar events may occur during HSP because nearby neighboring synapses have significantly higher differences in AMPAR homeostatic responses compared to the relative differences of more separated synapses. During HSP, the more drastic differences in AMPAR up-regulation between neighboring synapses may be resulted from preferential recruitment of AMPARs from the dendritic shaft to the spines. Or, given the involvement of protein synthesis, especially dendritic local protein synthesis, in AMPAR homeostatic up-regulation (Sutton et al. 2006), it is possible that the neighboring synapses compete for subcellular machinery for local AMPAR synthesis during HSP. Also, we observed that stronger increases in AMPAR amount occurring at the dendritic branching sites, consistent with the idea of these sites serving as storage pools of machinery for protein synthesis and trafficking (Horton and Ehlers 2003, Horton et al. 2005).

In summary, our findings provide the first piece of direct evidence supporting a non-scaling model for AMPAR up-regulation during HSP. Given that synaptic scaling is considered to be a necessary measure for information retention at the synaptic level which is crucial for memory, our findings of non-scaling HSP demands new mechanisms to enable the neural

circuits to keep memory information for an extended period of time. Obviously, there is a necessity for further in-depth investigations to unravel more detailed molecular steps and physiological implications of the non-scaling regulation in homeostatic synaptic plasticity. Moreover, the experimental methods we employed in this study could also be tested in other classic HSP paradigms, such as the prolonged TTX treatment-induced homeostatic up-scaling, and bicuculline-induced synaptic down-scaling. Of course, a lack of scaling in AMPAR synaptic accumulation does not completely exclude the possibility of scaling in synaptic activity because other factors, such as presynaptic transmitter release or postsynaptic receptor modifications, may compensate for the randomness in receptor number changes so as still able to achieve the functional scaling.

METHODS AND MATERIALS

Primary culture of rat hippocampal neurons

Primary hippocampal neurons were dissected from embryonic day 18 (E18) Sprague-Dawley rat fetuses and cultured as described previously (Wang et al. 2015). Briefly, brain tissues were digested and neural cells were dissociated with papain [0.5 mg/mL in Hank's balanced salt solution (HBSS), 37 °C for 20 minutes] then plated on 60-mm Petri dish containing five circular coverslips (18-mm diameter, 0.1-mm thickness) pre-coated in 0.1% poly-L-lysine to promote cellular adhesion. After dissociation, neural cells are counted and 0.6×10^6 cells were plated in a Petri dish. The cells are hence allowed to grow in plating medium (minimum essential media [MEM] containing 10% fetal bovine serum [FBS], 5% horse serum [HS], 31 mg L-cysteine, and 1% penicillin/streptomycin and L-glutamine mixture [1% P/S/G]; Invitrogen) overnight then switched into feeding medium (Neurobasal medium supplemented with 1% HS, 2% B-27, and 1% P/S/G; Gibco) for another 11 days before transfection. Cultured neural cells were fed twice a week by 1 mL feeding medium with supplement of 10 μM deoxyfluoruridine (FDU) to maintain their normal growth and development.

Neuronal cells transfection

Hippocampal neurons were transfected with Lipofectamine 2000 (Life technologies) on its day DIV 11 following the instruction of the manufacturer. For each 60-mm Petri dish, 5 μg GFP-GluA1, GFP-GluA2 or pH-GluA1 plasmid and 5 μL Lipofectamine 2000 were used for transfection. Briefly, the plasmid and Lipofectamine 2000 were placed in separated 1.5 mL Eppendorf tubes with 250 μL 1X MEM medium for 5 minutes then mixed together for another 20 minutes to form the transfection complex. Thereafter, the transfection complex was slowly added into the 60-mm Petri dish with 2.5 mL feeding medium in a drop-wise manner. The hippocampal neurons were hence incubated with the transfection complex at 37ºC for 4 hr before the medium replacement. The related proteins are allowed to express for another 72 hr before the live-cell imaging experiment being performed.

Immunostaining in cultured hippocampal neurons

Hippocampal neurons with GFP-GluA1, GFP-GluA2 or pH-GluA1 expressed were fixed for 10 minutes in 4% paraformaldehyde 4% sucrose solution on ice. After rinsing with 1X phosphate buffered saline (PBS), the cells were permeabilized with 0.3% Triton X-PBS

solution at room temperature for 8 minutes. After rinsing with PBS, the cells were then blocked in 10% goat serum for 1 hr and incubated with the primary antibody of the target proteins for another 2 hr with 5% goat serum present at room temperature. After rinsing, the cells were incubated for an additional hour with the Alexa Fluor-conjugated fluorescent secondary antibody (1:700 dilution). Cells were then rinsed and mounted to microscopy glass slides with Prolong Gold anti-fade mounting reagent (Life Technologies) and stored at 4°C for subsequent imaging.

Live-imaging of GFP-tagged synaptic AMPAR in cultured hippocampal neurons

Live-imaging of GFP-tagged synaptic AMPAR was conducted on a Carl Zeiss inverted fluorescent microscope with a temperature controller (Tempcontrol 37–2 digital) maintained at 37°C. To avoid the potential bias, neurons used in an individual set of experiments are from the same batch of cell culture preparation. Only the best-transfected and heathy neurons were chosen for analysis from each experiment. Cells morphologically identified as pyramidal neurons were chosen for imaging, and only the clearly transfected and healthy neurons were used for data analysis. Neurons in each condition came from 7–10 sets of experiments. Images were collected with a 63X oil-immersion objective (numerical aperture 1.4) before and after the 4 hr treatment with vehicle or APV + TTX. A blue glass filter was used to minimize the bleaching of GFP fluorescence in the process of imaging. The exposure time was manually adjusted to ensure the signal intensity is within the full dynamics range by using the glow lookup table in AxioVision Software (Release 4.5) provided by Carl Zeiss. Once the exposure time is established, it was used throughout all the images collected during the experiment. Based on the immunostaining results (Fig. 1B and Fig. S1), the vast majority (>99%) of GFP-GluA1, GFP-GluA2 or pH-GluA1 puncta analyzed in our experiments are synaptic. A small number of non-synaptic puncta may be included in the analysis.

Synaptic GFP-tagged AMPAR quantification and analysis

Images collected from live-imaging experiments were quantified and analyzed with NIH Image-J program. The plots and bar graphs of data were created in Microsoft Excel 2013 software. To quantify the relative GFP-GluA1, GFP-GluA2 or pH-GluA1 protein amount in individual punctum, the images were zoomed into 1600% then the edge of each punctum is clearly labeled manually by experienced researchers. The size and fluorescence intensity of each punctum were quantified by NIH Image J program then multiplied to generate the relative total amount of the related synaptic protein. The background fluorescence of each image is subtracted from the total fluorescence of the puncta before the multiplying. The relative changes of synaptic GFP-GluA1, GFP-GluA2 and pH-GluA1 are exhibited as the ratio of total protein amounts before and after the 4-hr vehicle or APV+TTX treatment.

The cumulative plots in Fig. 4 and Fig. S4 were generated following the conventional methods (Turrigiano et al. 1998). GFP-GluA1, GFP-GluA2 or pH-GluA1 puncta values from the pre-treatment (APV+TTX 0h) and the post-treatment (APV+TTX 4h) were considered as two independent data sets for ranked plotting (the black dots). The same data sets were then re-plotted in which the corresponding pre- and post-treatment values of individual puncta were matched (the color dots).

6. Statistics

Depending on the statistical properties of each experiment, Student's *t* test, Kolmogorov-Smirnov test, or mixed effect regression model have been used in this study. To account for the correlated size and distance measurements obtained from the same cell, we used linear mixed effect regression models with a random intercept assigned to each cell (Model 1).

$$Y_{ij} = \beta_0 + \beta_1 X_{1ij} + b_i + \varepsilon_{ij} \quad \text{(Model 1)}$$

Y_{ij} was the ratio of synaptic GFP-GluA1, GFP-GluA2 or pH-GluA1 protein amounts pre- and post-treatment on cell i at observation j; β_0 was the overall intercept; b_i was the separate random intercept for cell i and $b_i \sim N(0, \Theta)$, $\varepsilon_{ij} \sim N(0, \sigma^2)$. X_{1ij} was the pre-existing sizes of the puncta for participant i at visit j. A compound symmetry covariance structure was decided upon after comparing Akaike information criterion among models with different covariance structures as well as examining the estimated residual covariance matrix in our data. In addition, we used a robust/sandwich estimator for variance to avoid covariance misspecification. Simple linear regression model was used to test the association between X and Y. A two-tailed P value < 0.05 was considered as statistically significant. All analyses were performed using SAS 9.4 (SAS Institute, Cary NC) and R statistical computing software (R Foundation for Statistical Computing, Vienna, Austria).

1. Synaptic AMPAR amounts are regulated at various proportions during HSP
2. Changes of AMPAR at individual synapses do not follow a scaling pattern during HSP
3. The basal synaptic AMPAR level is inversely correlated to the extent of HSP response
4. Neighboring synapses compete for AMPAR during HSP

Supplementary Material

Refer to Web version on PubMed Central for supplementary material.

ACKNOWLEDGEMENTS

We would like to thank Dr. Margaret Hastings for comments on the manuscript and the Man Lab members for helpful discussion. This work was supported by NIH grant R01 MH079407 (H.Y.M.) and International Fulbright Sci & Tech Outstanding Student Award (G.W.). The authors declare no conflicts of financial interests.

REFERENCES

Aoto J, et al. 2008 Synaptic signaling by all-trans retinoic acid in homeostatic synaptic plasticity. Neuron 60, 308–320. [PubMed: 18957222]

Barnes SJ, et al. 2017 Deprivation-Induced Homeostatic Spine Scaling In Vivo Is Localized to Dendritic Branches that Have Undergone Recent Spine Loss. Neuron 96, 871–882 e875. [PubMed: 29107520]

Beique JC, et al. 2011 Arc-dependent synapse-specific homeostatic plasticity. Proc. Natl. Acad. Sci. U S A 108, 816–821. [PubMed: 21187403]

Blackman MP, et al. 2012 A critical and cell-autonomous role for MeCP2 in synaptic scaling up. J. Neurosci 32, 13529–13536. [PubMed: 23015442]

Davis GW 2006 Homeostatic control of neural activity: from phenomenology to molecular design. Annu. Rev. Neurosci 29, 307–323. [PubMed: 16776588]

Davis GW, Bezprozvanny I 2001 Maintaining the stability of neural function: a homeostatic hypothesis. Annu. Rev. Physiol 63, 847–869. [PubMed: 11181978]

Diering GH, Huganir RL 2018 The AMPA Receptor Code of Synaptic Plasticity. Neuron 100, 314–329. [PubMed: 30359599]

Echegoyen J, et al. 2007 Homeostatic plasticity studied using in vivo hippocampal activity-blockade: synaptic scaling, intrinsic plasticity and age-dependence. PLoS One 2, e700. [PubMed: 17684547]

Fernandes D, Carvalho AL 2016 Mechanisms of homeostatic plasticity in the excitatory synapse. J. Neurochem 139, 973–996. [PubMed: 27241695]

Fong MF, et al. 2015 Upward synaptic scaling is dependent on neurotransmission rather than spiking. Nat. Commun 6, 6339. [PubMed: 25751516]

Gilbert J, et al. 2016 beta-Amyloid triggers aberrant over-scaling of homeostatic synaptic plasticity. Acta Neuropathol. Commun 4, 131. [PubMed: 27955702]

Govindarajan A, et al. 2011 The dendritic branch is the preferred integrative unit for protein synthesis-dependent LTP. Neuron 69, 132–146. [PubMed: 21220104]

Govindarajan A, et al. 2006 A clustered plasticity model of long-term memory engrams. Nat. Rev. Neurosci 7, 575. [PubMed: 16791146]

Horton AC, Ehlers MD 2003 Dual modes of endoplasmic reticulum-to-Golgi transport in dendrites revealed by live-cell imaging. J. Neurosci 23, 6188–6199. [PubMed: 12867502]

Horton AC, et al. 2005 Polarized secretory trafficking directs cargo for asymmetric dendrite growth and morphogenesis. Neuron 48, 757–771. [PubMed: 16337914]

Hou Q, et al. 2011 Homeostatic regulation of AMPA receptor trafficking and degradation by light-controlled single-synaptic activation. Neuron 72, 806–818. [PubMed: 22153376]

Hou Q, et al. 2015 MicroRNA miR124 is required for the expression of homeostatic synaptic plasticity. Nat. Commun 6, 10045. [PubMed: 26620774]

Hou Q, et al. 2008 Homeostatic regulation of AMPA receptor expression at single hippocampal synapses. Proc. Natl. Acad. Sci. U S A 105, 775–780. [PubMed: 18174334]

Ibata K, et al. 2008 Rapid synaptic scaling induced by changes in postsynaptic firing. Neuron 57, 819–826. [PubMed: 18367083]

Jewett KA, et al. 2018 Dysregulation and restoration of homeostatic network plasticity in fragile X syndrome mice. Neuropharmacology 138, 182–192. [PubMed: 29890190]

Kim J, et al. 2012 An improved test for detecting multiplicative homeostatic synaptic scaling. PLoS One 7, e37364. [PubMed: 22615990]

Lee KY, et al. 2018 Loss of fragile X protein FMRP impairs homeostatic synaptic downscaling through tumor suppressor p53 and ubiquitin E3 ligase Nedd4–2. Hum. Mol. Gene 27, 2805–2816.

Matsubara T, Uehara K 2016 Homeostatic Plasticity Achieved by Incorporation of Random Fluctuations and Soft-Bounded Hebbian Plasticity in Excitatory Synapses. Front. Neural. Circuits 10, 42. [PubMed: 27313513]

Pozo K, Goda Y 2010 Unraveling mechanisms of homeostatic synaptic plasticity. Neuron 66, 337–351. [PubMed: 20471348]

Pratt KG, et al. 2011 Presenilin 1 regulates homeostatic synaptic scaling through Akt signaling. Nat. Neurosci 14, 1112. [PubMed: 21841774]

Shepherd JD, et al. 2006 Arc/Arg3.1 mediates homeostatic synaptic scaling of AMPA receptors. Neuron 52, 475–484. [PubMed: 17088213]

Soares C, et al. 2013 Differential subcellular targeting of glutamate receptor subtypes during homeostatic synaptic plasticity. J. Neurosci 33, 13547–13559. [PubMed: 23946413]

Stellwagen D, Malenka RC 2006 Synaptic scaling mediated by glial TNF-alpha. Nature 440, 1054–1059. [PubMed: 16547515]

Styr B, Slutsky I 2018 Imbalance between firing homeostasis and synaptic plasticity drives early-phase Alzheimer's disease. Nat. Neurosci 21, 463–473. [PubMed: 29403035]

Sutton MA, et al. 2006 Miniature neurotransmission stabilizes synaptic function via tonic suppression of local dendritic protein synthesis. Cell 125, 785–799. [PubMed: 16713568]

Turrigiano G 2011 Too many cooks? Intrinsic and synaptic homeostatic mechanisms in cortical circuit refinement. Annu. Rev. Neurosci 34, 89–103. [PubMed: 21438687]

Turrigiano GG 2008 The self-tuning neuron: synaptic scaling of excitatory synapses. Cell 135, 422–435. [PubMed: 18984155]

Turrigiano GG, et al. 1998 Activity-dependent scaling of quantal amplitude in neocortical neurons. Nature 391, 892–896. [PubMed: 9495341]

Vitureira N, et al. 2012 Homeostatic synaptic plasticity: from single synapses to neural circuits. Curr. Opin. Neurobiol 22, 516–521. [PubMed: 21983330]

Wang G, et al. 2015 Resveratrol up-regulates AMPA receptor expression via AMP-activated protein kinase-mediated protein translation. Neuropharmacology 95, 144–153. [PubMed: 25791529]

Wang G, et al. 2012 AMPA receptor trafficking in homeostatic synaptic plasticity: functional molecules and signaling cascades. Neural Plast 2012, 825364. [PubMed: 22655210]

Wierenga CJ, et al. 2005 Postsynaptic expression of homeostatic plasticity at neocortical synapses. J. Neurosci 25, 2895–2905. [PubMed: 15772349]

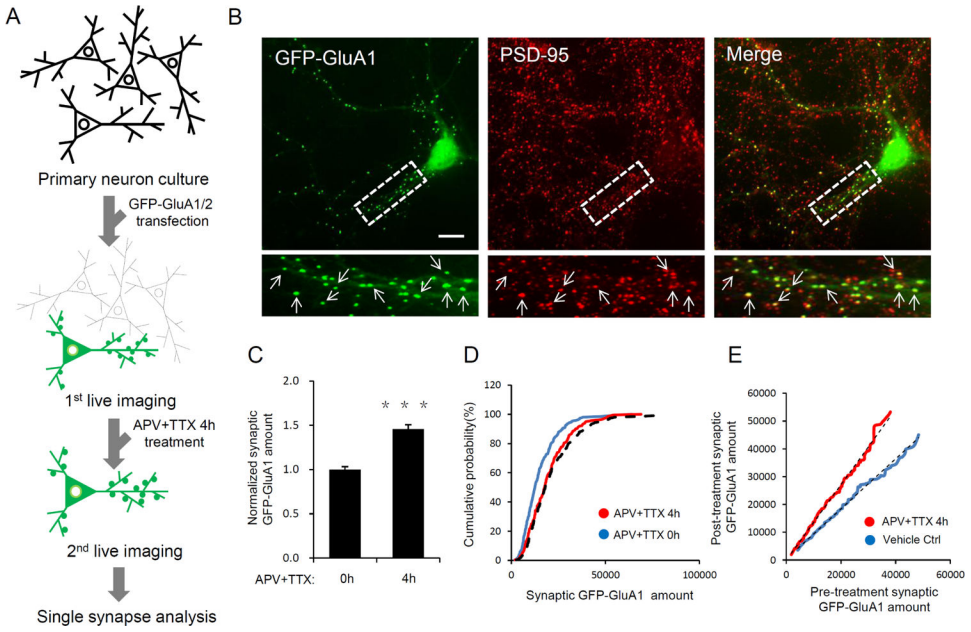

Fig. 1. Live-imaging shows inactivity-induced homeostatic up-regulation of AMPARs at individual synapses.

(A) A schematic illustration of the experimental paradigm. Cultured rat hippocampal neurons were transfected to express GFP-GluA1, GFP-GluA2 or pH-GluA1, respectively, from day *in vitro* (DIV) 11–14. Neurons were then imaged before and immediately after 4 hr incubation with APV (50 μM) and TTX (2 μM). (B) Immunostaining of synaptic protein PSD95 (red) showed localization of GFP-GluA1 puncta (green) at the synaptic sites. (C) Pooled data showed that 4 hr treatment with APV+TTX resulted in a significant homeostatic increase in synaptic GFP-GluA1 amount (1.43 ± 0.06, n = 985 puncta of 30 neurons). (D, E) Conventional cumulative (D) and ranked (E) plotting of GFP-GluA1 puncta intensities revealed proportional up-scaling of synaptic AMPARs. The dashed line in black, which fits well with the red curve (APV+TTX 4h), was generated by multiplying the average GFP-GluA1 increase (1.43) to the values of blue curve (APV+TTX 0h). Bar graph represents Mean ± S.E. ***$P < 0.001$. Two-tailed student's t test. Scale bar, 20 μm.

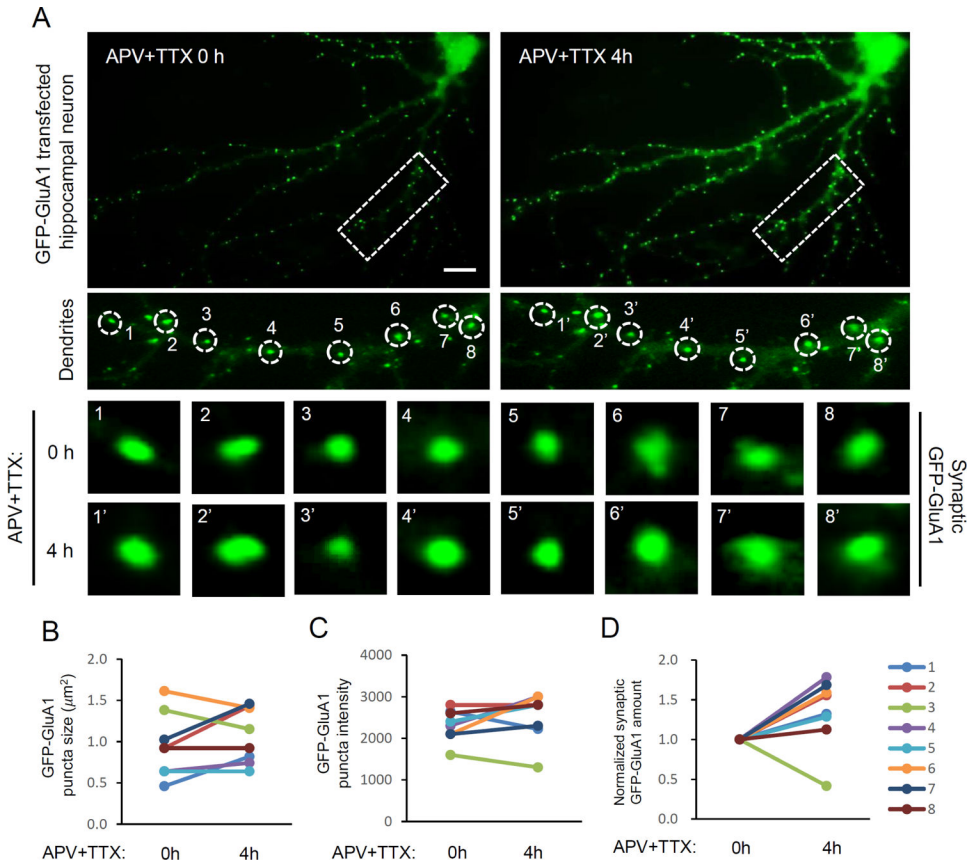

Fig. 2. GFP-GluA1 puncta show non-scaling pattern during homeostatic synaptic plasticity.

(A) Representative images of a neuron expressing GFP-GluA1, before and after the APV +TTX 4 h treatment. Eight individual GFP-GluA1 puncta on a dendrite were shown prior to and after the treatment. (B-D) Analysis of the 8 individual GFP-GluA1 puncta showed different levels of changes in puncta size (B), mean intensity (C) and normalized total protein amount (D), indicating non-uniform regulation of AMPAR accumulation at individual synapses. Scale bar, 20 μm.

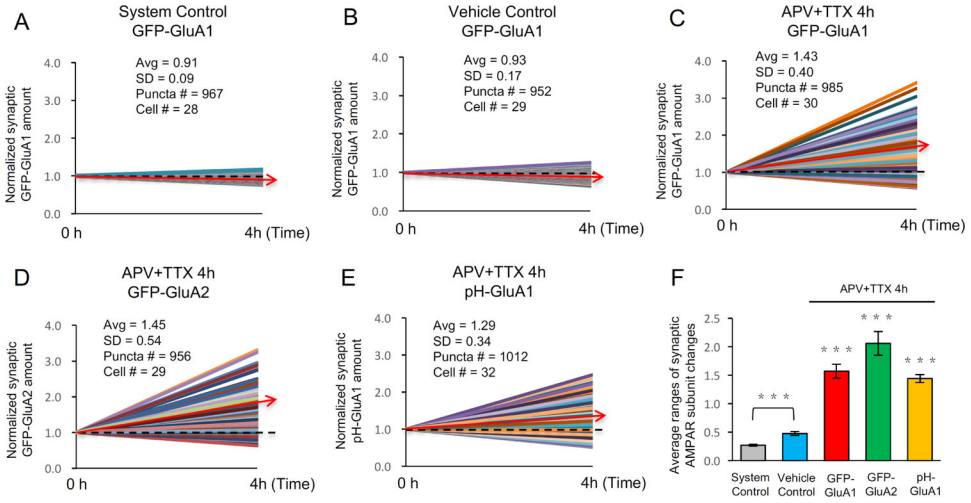

Fig. 3. Synaptic AMPARs show a wide range of alterations during homeostatic synaptic plasticity.

(A-E) Synapses in system (A) and vehicle (B) controls showed minimal and random alterations in AMPAR amounts over the 4 hr period, whereas synapses in APV+TTX treated groups showed scattered patterns of overall up-regulation (C-E). The red arrow line indicates the mean value of each group. (F) The ranges of changes in synaptic GFP-GluA1, GFP-GluA2 and pH-GluA1 in APV+TTX treated neurons were significantly larger than those of system or vehicle control ($n = 28$ 32 neurons per group). Bar graph represents Mean ± S.E. ***$P < 0.001$. Two-tailed student's t test.

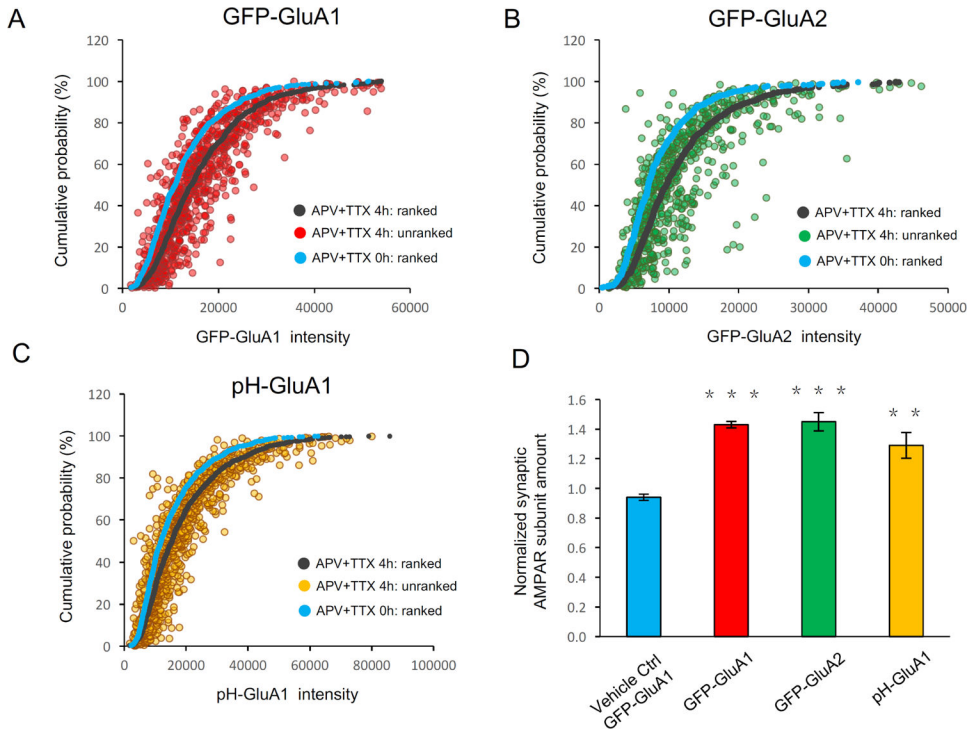

Fig. 4. Scattered pattern of homeostatic up-regulation of AMPARs at individual synapses.

(A-C) Quantification of individual AMPAR subunit puncta shows a clear scattered pattern of AMPAR up-regulation during HSP. The color dots are individual synaptic AMPAR subunit amounts after induction of HSP (APV+TTX 4h) displayed in an unranked manner (red: GFP-GluA1, A; green: GFP-GluA2, B; yellow: pH-GluA1, C), while the black curves are the same sets of data plotted in a ranked manner. Blue curves are the individual synaptic AMPAR subunit amounts before HSP (APV+TTX 0h) plotted in a ranked manner. Statistical significance between pre- and post-treatment of GFP-GluA1 (A), GFP-GluA2 (B), or pH-GluA1 (C) was verified with the Kolmogorov-Smirnov test. P's < 0.001. (D) Pooled data showed homeostatic increase in synaptic amounts of GFP-GluA1 (red, 1.43 ± 0.06), GFP-GluA2 (green, 1.45 ± 0.09) and pH-GluA1 (yellow, 1.29 ± 0.06). Bar graph represents Mean ± S.E., ***$P < 0.001$, **$P < 0.01$. Two-tailed student's t test.

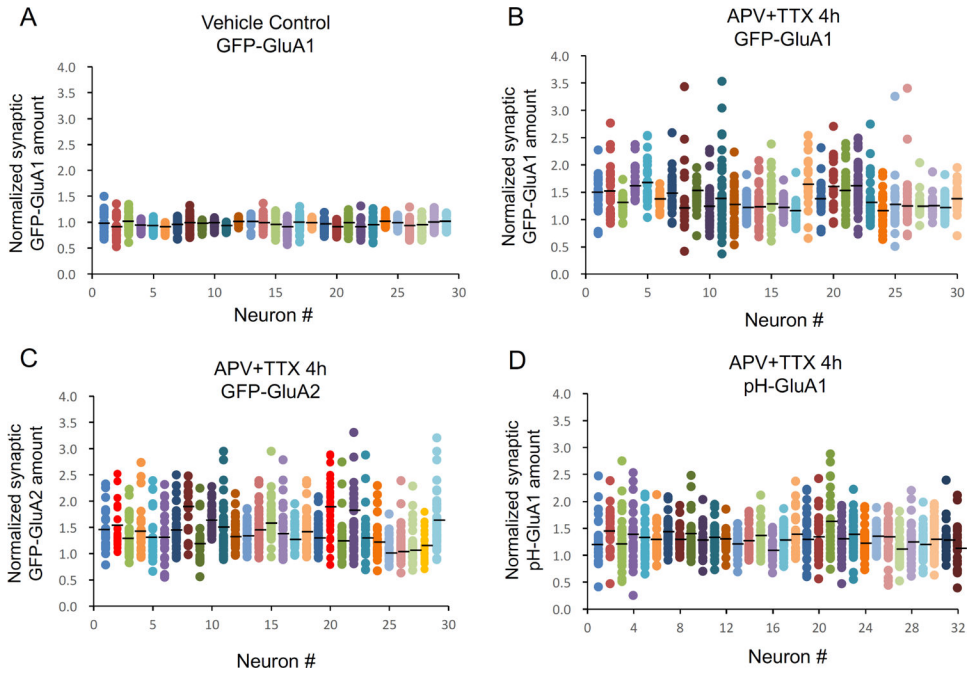

Fig. 5. Scattered homeostatic regulation of synaptic AMPARs in individual neurons.

A dot represents a single GFP-GluA1, GFP-GluA2 or pH-GluA1 punctum in individual neurons, which were color-coded in columns (Vehicle control: n = 952 puncta from 29 neurons; GFP-GluA1: n = 985 puncta from 30 neurons; GFP-GluA2: n = 956 puncta from 29 neurons; pH-GluA1: n = 1012 puncta from 32 neurons). The horizontal black bar in each column indicates the average synaptic AMPAR change of each neuron.

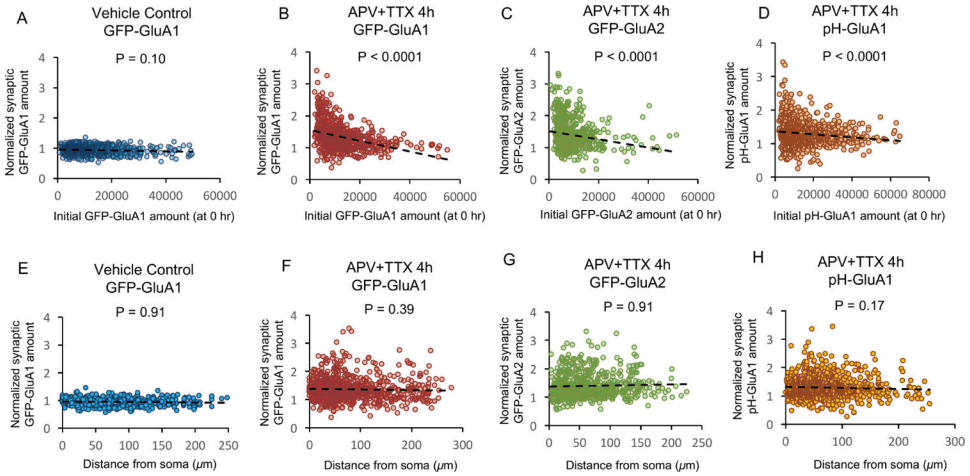

Fig. 6. Relationship of synaptic AMPAR homeostatic response with basal protein level and dendritic localization.

(A-D) Data analysis showed that the initial amount of synaptic GFP-GluA1, GFP-GluA2 or pH-GluA1 is inversely correlated to its strength of homeostatic response. (E-H) Data analysis showed a lack of correlation between puncta localizations relative to the soma and the extent of homeostatic changes. Mixed effect regression model was used for significance test.

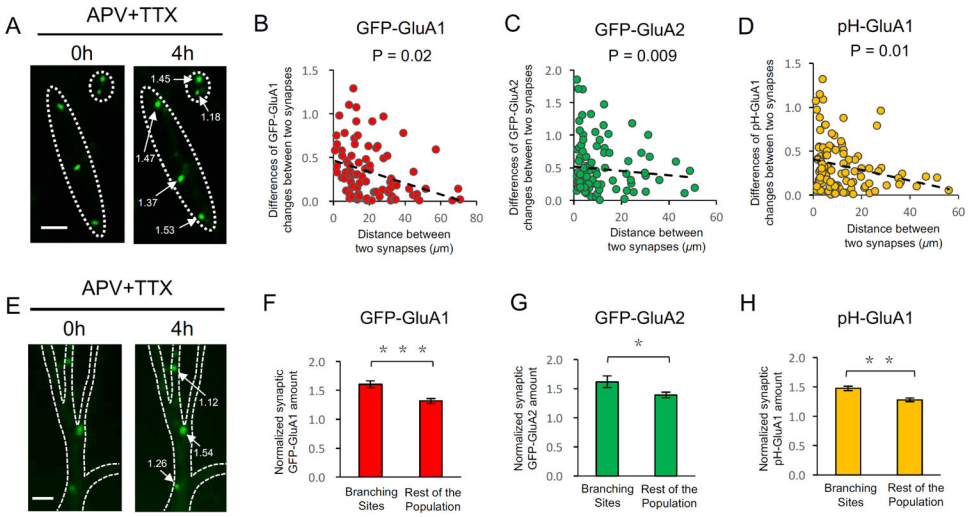

Fig. 7. Competition between neighboring synapses in AMPAR homeostatic regulation.

(A) Representative GFP-GluA1 puncta with varied inter-puncta distance. Receptor puncta were distributed either closely (the small dashed line circle) or in a more separated pattern (the bigger dashed line circle). (B-D) In GFP-GluA1 (B), GFP-GluA2 (C) and pH-GluA1(D), the difference of AMPAR up-regulation during HSP between two neighboring synapses is negatively correlated with their separation distance. (E) Representative GFP-GluA1 puncta at the branching sites of dendrites. (F-H) AMPARs at the branching sites of dendritic shaft were regulated to higher levels compared to those distributed at the non-branching sites of the same neurons (GFP-GluA1: 1.60 ± 0.06 vs. 1.32 ± 0.04, n = 159 puncta of 19 neurons, F; GFP-GluA2: 1.62 ± 0.1 vs. 1.39 ± 0.05, n = 143 puncta of 18 neurons, G; pH-GluA1: 1.48 ± 0.04 vs. 1.28 ± 0.03, n = 165 puncta of 20 neurons, H). The values in the images indicate changes in synaptic AMPAR induced by APV+TTX 4h treatment. Mixed effect regression model (B-D) and two-tailed student's *t* test (F-H) were used for significance test. $*P < 0.05$, $**P < 0.01$, $***P < 0.001$. Scale bar, 5 μm.